

## Selection of eutectic structure

E. A. Brener, M. B. Geřlikman, and D. E. Temkin

*Institute of Experimental Mineralogy, Academy of Sciences of the USSR*

(Submitted 16 April 1986)

Zh. Eksp. Teor. Fiz. **92**, 165–178 (January 1987)

The selection of a structure during the eutectic crystallization of a thin film is studied. This selection occurs as a result of a competition between the appearance and disappearance of lamellae. Equations of motion are constructed for an irregular structure. They are analyzed in the long-wave approximation, in which it is assumed that the length scales of the structural irregularities are greater than the lamellar spacing  $\lambda_0$ . The size distribution of the lamellae is found as a function of the parameters of the growth process and the noise level. As the composition of the initial phase deviates progressively further from the eutectic composition, a transition takes place to the growth of a random structure, characterized by a high frequency of events in which lamellae appear and disappear. The period of the selected structure,  $\lambda_0$ , can fall anywhere in an interval of values, depending on the particular model adopted for the splitting of the lamellae. This interval is found. Its lower boundary is derived under the assumption that the splitting of the lamellae occurs primarily at the size corresponding to the maximum of the distribution function. The upper boundary of the interval corresponds to the splitting of lamellae at the point at which the crystallization front becomes unstable. For the Pb-Sn eutectic system, this interval is  $1.4 < \lambda_0/\lambda_m < 2.2$ , where  $\lambda_m$  is the lamellar spacing corresponding to the minimum of the supercooling at the given growth rate. The experimental values are in the interval  $1.2 < \lambda_0/\lambda_m < 2.0$ .

### INTRODUCTION

The evolution of an inhomogeneous state of a nonequilibrium system and the mechanisms by which its pattern is selected have recently been the subject of active research, including some research pertinent to crystallization processes.<sup>1,2</sup> A general characteristic feature of such processes as the growth of dendrites, eutectic crystallization, and cellular crystallization is the existence of a range of inhomogeneous states which may arise in the course of the process. The problem here is to describe the time evolution of an inhomogeneous state and ultimately to determine the parameters of the structure which is realized after a long time. The theory of steady-state eutectic growth<sup>3,4</sup> predicts only a relationship between the growth velocity and the lamellar spacing  $\lambda$  of a regular structure:

$$V(\lambda) \sim \frac{\Delta T}{\lambda} \left( 1 - \frac{\lambda_c(\Delta T)}{\lambda} \right).$$

Alternatively, if we are dealing with crystallization at a fixed rate in a temperature gradient, this theory predicts a relationship between the parameter  $\lambda$  and the supercooling at the crystallization front,  $\Delta T$ . In order to determine which value of  $\lambda$  actually prevails during the growth of the eutectic, it is thus necessary to appeal to other considerations.

We first note that, as was pointed out by J. W. Cahn and discussed by Jackson and Hunt,<sup>4</sup> steady growth will be unstable under the condition  $\lambda < 2\lambda_c$ , where  $\lambda = 2\lambda_c$  is the point of the maximum on the  $V(\lambda)$  curve. On the other hand, as Jackson and Hunt pointed out,<sup>4</sup> an instability of another type arises if  $\lambda$  is sufficiently large. The crystallization front bends near a lamella, forming deep "pockets," with the result that initiation of a lamella of a second solid phase becomes possible. A hypothesis of marginal growth was then formulated. This is the assertion that the growth occurs under conditions corresponding to a stability boundary. Langer<sup>5</sup> confirmed the result  $\lambda = 2\lambda_c$ , which corre-

sponds to an instability of the first type and which agrees with the earlier suggestion<sup>6</sup> of a maximum of the velocity (or a minimum of the supercooling). Sundquist<sup>7</sup> has suggested that  $\lambda$  corresponds to a threshold for an instability with respect to the nucleation of new lamellae, i.e., an instability of the second type. The condition that the derivative of the entropy reach a maximum and also certain auxiliary considerations<sup>8</sup> lead to a different result,  $\lambda = 3\lambda_c$ , which corresponds to an inflection point on the  $V(\lambda)$  curve. Finally, Datye *et al.*<sup>9</sup> formulated a systematic approach to the analysis of selection based on the two types of structural instabilities mentioned above, at small and large values of  $\lambda$ . The first of these instabilities leads to the disappearance of lamellae of small dimensions, with the result that the structure becomes coarser. An instability of lamellae of sufficiently large dimensions results in their splitting and thus the creation of new lamellae. This process has the opposite result of reducing the average lamellar spacing  $\lambda$ . The steady-state structure which arises as a result of the selection corresponds to a dynamic equilibrium between these processes of the splitting and termination of lamellae. The evolution and the selection of a eutectic structure is a many-body problem; the effective interaction between lamellae occurs through a diffusion field in the melt. Since this problem is so complex, it is useful to construct some simple but physically meaningful models. To describe the dynamics of a eutectic structure, Datye *et al.*<sup>9</sup> accordingly used a simplified model in which the evolution of the structure results from curvature of the macroscopic crystallization front which runs along triple junctions of lamellae with the melt. Here it was postulated that the lamellae are perpendicular to the line of the macroscopic front. So far, no justification has been found for this postulate. Datye *et al.*<sup>9</sup> wrote an equation for  $\lambda(x,t)$  in the long-wave approximation, according to which the local supercooling at the front,  $\Delta T(\lambda)$ , depends only on the local value of  $\lambda$ , not on the average characteristics of the structure:

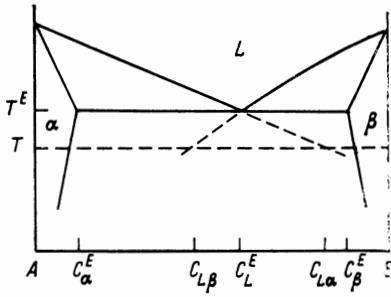


FIG. 1. Eutectic phase diagram.

$$\lambda \sim \partial^2(\Delta T(\lambda))/\partial x^2.$$

The problem nevertheless remains a many-body problem.

In the present paper we consider the situation in which the additional assumption that the lamellae are perpendicular to the macroscopic front is not required. Specifically, if the surface energy between the melt and the solid phases is large in comparison with the surface energy of the boundary between solid phases, then—as we will see below—we can ignore the curvature of the macroscopic front, and the evolution and thus structure selection will occur at a macroscopically planar front. Assuming this front to be statistically uniform, and using the long-wave description, we find a single-particle equation of motion,  $\lambda = f(\lambda)$ , but one which depends on the average structural characteristics as parameters. Also incorporating the fluctuations which arise in the system in the analysis, we describe the process of the evolution and selection of a structure, allowing for the disappearance and appearance of lamellae. As a result we find the mean value and variance of the lamellar spacing in a eutectic structure. We compare the results with experimental data.

### EQUATIONS FOR THE GROWTH OF AN IRREGULAR EUTECTIC

We consider the isothermal crystallization of a thin film in a eutectic system with the phase diagram shown schematically in Fig. 1. Figure 2 shows the structure of the solid phase, which consists of alternating  $\alpha$  and  $\beta$  lamellae. This process is controlled by diffusive redistribution of the components in the liquid phase and is described by the two-dimensional diffusion equation

$$\frac{\partial C_L}{\partial t} = D \left( \frac{\partial^2 C_L}{\partial x^2} + \frac{\partial^2 C_L}{\partial z^2} \right), \quad (1)$$

where  $C_L$  is the atomic fraction of component B, and  $D$  is the interdiffusion coefficient in the melt. We ignore diffusion in

the solid phase. At the crystallization front,  $z = \xi(x, t)$  matter is conserved:

$$\frac{\partial C_L}{\partial n} = \frac{v_n}{D} (C_s - C_L) \quad (S = \alpha, \beta), \quad (2)$$

where  $v_n = (\partial \xi / \partial t) / [1 + (\partial \xi / \partial x)^2]^{1/2}$  is the normal growth velocity,  $\partial C_L / \partial n$  is the derivative along the normal to the front, and  $C_s$  is the composition of the crystal, which is equal to  $C_\alpha^E$  in an  $\alpha$  lamella or  $C_\beta^E$  in a  $\beta$  lamella. We also assume that the conditions of a local equilibrium hold at the curved front:

$$C_L - C_{L\alpha} - \Gamma_\alpha K = 0 \quad \text{at an } \alpha \text{ lamella}, \quad (3a)$$

$$C_L - C_{L\beta} + \Gamma_\beta K = 0 \quad \text{at a } \beta \text{ lamella}, \quad (3b)$$

where  $K$  is the local curvature,  $C_{L\alpha}$  and  $C_{L\beta}$  are the equilibrium compositions on the continuation of the liquidus lines (Fig. 1), and  $\Gamma_\alpha$  and  $\Gamma_\beta$  are capillary lengths,<sup>10</sup> given by

$$\Gamma_s = \sigma_{LS} \Omega_s / f_L''(C_s^E) |C_s^E - C_L^E|, \quad S = \alpha, \beta. \quad (3c)$$

Here  $\sigma_{LS}$  is the specific free energy of the interface between the  $L$  and  $S$  phases,  $\Omega_s$  is the atomic volume and  $f_L''$  is the second derivative with respect to the composition of the free energy per atom of the liquid phase (the derivative is taken at the eutectic point). The meanings of the various compositions are explained by Fig. 1.

The equilibrium conditions at the triple junctions,

$$\sigma_{L\alpha} \sin \theta_\alpha + \sigma_{L\beta} \sin \theta_\beta = \sigma_{\alpha\beta}, \quad \sigma_{L\alpha} \cos \theta_\alpha = \sigma_{L\beta} \cos \theta_\beta$$

determine the angles  $\theta_\alpha$  and  $\theta_\beta$  (Fig. 2);  $\sigma_{\alpha\beta}$  is the free energy of the interface between the  $\alpha$  and  $\beta$  phases. The inclination of the front at the triple junctions is determined by the relations

$$\partial \xi / \partial x = -\tan(\theta_\alpha + \theta_\beta) \quad \text{at } x = x_i - 0, \quad (4a)$$

$$\partial \xi / \partial x = \tan(\theta_\beta - \theta_\alpha) \quad \text{at } x = x_i + 0, \quad (4b)$$

where  $\sigma_i$  is the inclination of the interface between the  $\alpha$  and  $\beta$  lamellae (Fig. 2a). Equations (1)–(4) along with the initial conditions determine the process by which the eutectic crystallizes.

The problem formulated above is extremely complicated. At this point we adopt the approximation of a plane crystallization front which is moving at a constant velocity  $V$  (Fig. 2b). In seeking the concentration field ahead of a growing irregular eutectic, we solve the diffusion equation in the coordinate system moving with the front. We consider boundary condition (2) at a plane front, i.e., at  $z = 0$  (Ref. 4).

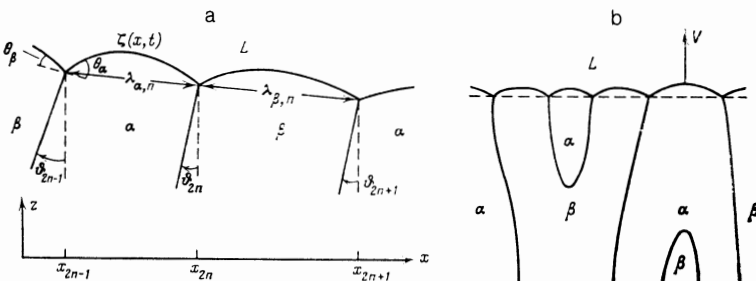


FIG. 2. Irregular lamellar structure. a—Region of curved macroscopic front; b—region of plane macroscopic front, where a  $\beta$  lamella is disappearing and an  $\alpha$  lamella is appearing.

The quasisteady approximation, in which a macroscopic crystallization front (a front drawn through triple points) is actually planar and is moving at a constant velocity  $V$ , can be based on the linear analysis of structural perturbations which was carried out in Ref. 11. At small values of the angles  $\theta_\alpha$  and  $\theta_\beta$  at a section of the front spanning a large number of lamella,  $n \sim 1/\theta \gg 1$ , with lamella dimensions which are essentially constant, it is found that a steady-state front with a shape only slightly different from planar can be established. If we consider a statistically uniform crystallization front (i.e., if we assume that the size distribution of the lamellae does not depend on the coordinate along the front), then we can assume that the front is planar and is moving at a velocity  $V$  which depends only on the mean characteristics of the eutectic structure.

In this case the concentration field found from the solution of (1) and (2) can be written

$$C_L = C_\infty + (\bar{C}_L - C_\infty) \exp(-Vz/D) + \bar{C}_L, \quad (5)$$

where  $\bar{C}_L$  is the mean composition along the crystallization front, and  $C_\infty$  is the initial composition of the melt far from the front.

If the supersaturation is small (and, correspondingly, if the growth velocity  $V$  is small), and if the length scales  $l$  of the structural irregularities are not too large ( $l/D < 1$ ), we can find  $\bar{C}_L$  from the steady-state diffusion equation,  $\Delta \bar{C}_L = 0$  and

$$\bar{C}_L(x, z=0) = \frac{V(C_\beta^E - C_\alpha^E)}{\pi D} \int_{-\infty}^{\infty} g(x') \ln|x-x'| dx'. \quad (6)$$

The function  $g(x)$  depends on the particular sequence of  $\alpha$  and  $\beta$  lamellae along the front:

$$g(x) = \begin{cases} g_\alpha \equiv -(1-\eta_0) & \text{at an } \alpha \text{ lamella,} \\ g_\beta \equiv \eta_0 & \text{at a } \beta \text{ lamella.} \end{cases} \quad (7)$$

Here  $\eta_0$  is the mean fraction of the  $\alpha$  phase, which can be found from the obvious relation

$$\eta_0 C_\alpha^E + (1-\eta_0) C_\beta^E = C_\infty.$$

Knowing the concentration distribution, we can work from Eqs. (3) and (4) to find the shape of the crystallization front. In particular, integrating (3) once, we find, for small values of  $\theta_s$  and  $\vartheta_i$ ,

$$\vartheta_{2n} - \vartheta_{2n-1} = -2\theta_\alpha - \frac{1}{\Gamma} \int_{x_{2n-1}}^{x_{2n}} [C_L(x) - C_{L\alpha}] dx, \quad (8a)$$

$$\vartheta_{2n+1} - \vartheta_{2n} = -2\theta_\beta + \frac{1}{\Gamma_\beta} \int_{x_{2n}}^{x_{2n+1}} [C_L(x) - C_{L\beta}] dx. \quad (8b)$$

At small angles  $\vartheta_i$ , the rate of change of the dimensions of the lamellae is

$$\dot{\lambda}_{\alpha, n} = V(\vartheta_{2n} - \vartheta_{2n-1}), \quad \dot{\lambda}_{\beta, n} = V(\vartheta_{2n+1} - \vartheta_{2n}). \quad (9)$$

Substituting relations (8) into (9), we finally find

$$\dot{\lambda}_{\beta, n} = V\{-2\theta_\beta + [\lambda_{\beta, n}(\bar{C}_L - C_{L\beta}) + J_{\beta, n}]/\Gamma_\beta\}, \quad (10)$$

$$J_{\beta, n} = \int_{\lambda_{\beta, n}} \bar{C}_L(x) dx, \quad (11)$$

where  $S = \alpha, \beta$ ; the upper sign refers to an  $\alpha$  lamella; and the lower sign refers to the  $\beta$  lamella.

At a plane crystallization front, two conservation conditions must hold. These conditions enable us to express  $\bar{C}_L$  and  $V$  in terms of the mean characteristics of the structure. The first conservation condition is the conservation of the total length of the macroscopic front:

$$\frac{d}{dt} \sum_n (\lambda_{\alpha, n} + \lambda_{\beta, n}) = 0.$$

The second condition guarantees that the mean composition of the solid phase be the same as the composition of the original melt:

$$\sum_n [C_\alpha^E \lambda_{\alpha, n} + C_\beta^E \lambda_{\beta, n} - C_\infty (\lambda_{\alpha, n} + \lambda_{\beta, n})] = 0.$$

These conditions are equivalent to the conditions  $\langle \dot{\lambda}_{\alpha, n} \rangle = \langle \dot{\lambda}_{\beta, n} \rangle = 0$ , from which we find

$$\langle J_{\alpha, n} \rangle = -\langle J_{\beta, n} \rangle = \eta_0 (1-\eta_0) (C_{L\alpha} - C_{L\beta}) \langle \lambda_n \rangle - 2(\Gamma_\beta \theta_\beta \eta_0 + \Gamma_\alpha \theta_\alpha (1-\eta_0)), \quad (12a)$$

$$\bar{C}_L = C_{L\beta} (1-\eta_0) + C_{L\alpha} \eta_0 + \frac{2}{\langle \lambda_n \rangle} (\Gamma_\beta \theta_\beta - \Gamma_\alpha \theta_\alpha). \quad (12b)$$

Here we have used

$$\int_{-\infty}^{\infty} \bar{C}_L(x) dx = 0, \quad \lambda_n = \lambda_{\alpha, n} + \lambda_{\beta, n},$$

and the angle brackets mean an average along the front. Equations (10) describe the dynamics of the structural transformation. An analysis of these equations in their general form is very complicated, so we will examine them in the long-wave approximation, to which we now turn.

#### EQUATIONS OF MOTION IN THE LONG-WAVE APPROXIMATION

In the case in which  $\lambda_{s, n}$  are slowly varying functions of  $n$  (or of the spatial coordinate  $x$ ), we write  $g(x)$  in (7) as the sum  $g(x) = \bar{g}(x) + \tilde{g}(x)$ , where

$$\bar{g}(x) = (g_\alpha \lambda_{\alpha, n} + g_\beta \lambda_{\beta, n})/\lambda_n \equiv -[\eta(x) - \eta_0], \quad (13a)$$

$$\tilde{g}(x) = \begin{cases} -[1 - \eta(x)] & \text{at an } \alpha \text{ lamella,} \\ \eta(x) & \text{at a } \beta \text{ lamella,} \end{cases} \quad (13b)$$

and  $\eta(x) = \lambda_\alpha(x)/\lambda(x)$ . The function  $\bar{g}(x)$  is the mean value of  $g$  over the period  $\lambda_n$ ; it varies slowly along the coordinate  $x$ . The function  $\tilde{g}(x)$  varies sharply at the transition from an  $\alpha$  lamella to a  $\beta$  lamella, but its mean value over the period  $\lambda_n$  is zero. From (6), and (13), we can put the concentration  $\bar{C}_L(x)$  in the form

$$\bar{C}_L(x) = \frac{V(C_\beta^E - C_\alpha^E)}{\pi D} \left\{ \int_{-\infty}^{\infty} dx' \bar{g}(x') \ln|x-x'| - \int_{-\infty}^{\infty} dx' [\eta(x') - \eta_0] \ln|x-x'| \right\}. \quad (14)$$

If we ignore the small terms which contain derivatives of  $\lambda_s(x)$ , we find that in calculating the integrals  $J_s(x)$  from (11) the first term in (14) makes the same contribution as in a regular eutectic, but with local values of  $\lambda_s(x)$ . The second term in (14) varies substantially over distances on the order

of the scale of the irregularities,  $l \gg \lambda$ , and it can be assumed constant in the evaluation of the integrals over  $\lambda_S$ . As a result we find

$$J_S(x) = \frac{V(C_{\beta}^{\#} - C_{\alpha}^{\#})}{D} \left[ \pm \lambda^2(x) P(\eta) - \frac{\lambda_S(x)}{\pi} \times \int_{-\infty}^{\infty} dx' [\eta(x') - \eta_0] \ln |x - x'| \right], \quad (15)$$

where

$$P(\eta) = \sum_{k=1}^{\infty} \frac{\sin^2 \pi k \eta}{(\pi k)^3}; \quad (16)$$

$S = \alpha, \beta$ ; the upper sign refers to  $S = \alpha$ ; and the lower sign to  $S = \beta$ . It can be seen from expression (15) that a substantial deviation from local behavior arises if the phase fraction  $\eta(x)$  deviates from its mean value  $\eta_0$ . This deviation from local behavior enters Eq. (10) for  $\lambda_{s,n}$ , so that one of the combinations of these two equations is purely local:

$$\frac{\Gamma_{\alpha}}{V\lambda_{\alpha}(x)} \dot{\lambda}_{\alpha}(x) + \frac{\Gamma_{\beta}}{V\lambda_{\beta}(x)} \dot{\lambda}_{\beta}(x) = (C_{L\alpha} - C_{L\beta}) - \frac{V}{D} (C_{\beta}^{\#} - C_{\alpha}^{\#}) \lambda^2(x) P(\eta) \left( \frac{1}{\lambda_{\alpha}(x)} + \frac{1}{\lambda_{\beta}(x)} \right) - \frac{2\Gamma_{\alpha}\theta_{\alpha}}{\lambda_{\alpha}(x)} - \frac{2\Gamma_{\beta}\theta_{\beta}}{\lambda_{\beta}(x)}. \quad (17)$$

The other, which describes  $\dot{\eta}(x)$ , reflects the nonlocal nature of this situation in a fundamental way. This nonlocal behavior implies that long-wave perturbations of  $\eta(x)$  relax rapidly to their average value  $\eta_0$ , and in describing the changes in  $\lambda$  we can set  $\eta = \eta_0$  in Eq. (17). To verify this assertion, we consider Eqs. (10) in the approximation linear in the deviations from the average values. Substituting the variables  $\Delta\eta = \eta - \eta_0$ ,  $\Delta\lambda = \lambda - \lambda_0$  in the form

$$\Delta\eta(x, t) = e^{-\omega t} \int_{-\infty}^{\infty} \frac{dk}{2\pi} e^{ikx} \Delta\eta_k, \quad \Delta\lambda(x, t) = e^{-\omega t} \int_{-\infty}^{\infty} \frac{dk}{2\pi} e^{ikx} \Delta\lambda_k,$$

into (10) and using (15), we find

$$\omega_{\lambda} \approx \frac{\lambda_0 V^2 (C_{\beta}^{\#} - C_{\alpha}^{\#}) P(\eta_0)}{D (\Gamma_{\alpha} + \Gamma_{\beta}) \eta_0 (1 - \eta_0)} \frac{(\lambda_0 - 2\lambda_c)}{(\lambda_0 - \lambda_c)}, \quad (18a)$$

$$\omega_{\eta} \approx \frac{1}{|k|} \frac{V^2 (C_{\beta}^{\#} - C_{\alpha}^{\#}) \eta_0 (1 - \eta_0) (\Gamma_{\alpha} + \Gamma_{\beta})}{D \Gamma_{\alpha} \Gamma_{\beta}}, \quad (18b)$$

where  $\lambda_0$  and  $\eta_0$  are average values.

It can be seen from (18a) that the eutectic structure is unstable in the case  $\lambda_0 < 2\lambda_c$ , where  $\lambda = 2\lambda_c$  is the point of the maximum on the  $V(\lambda)$  curve which describes the growth velocity of a regular eutectic<sup>4</sup>:

$$V(\lambda) = \frac{D}{\lambda} \frac{(C_{L\alpha} - C_{L\beta}) \eta_0 (1 - \eta_0) (1 - \lambda_c/\lambda)}{(C_{\beta}^{\#} - C_{\alpha}^{\#}) P(\eta_0)}, \quad (19a)$$

$$\lambda_c = \frac{1}{(C_{L\alpha} - C_{L\beta})} \left( \frac{2\Gamma_{\alpha}\theta_{\alpha}}{\eta_0} + \frac{2\Gamma_{\beta}\theta_{\beta}}{1 - \eta_0} \right). \quad (19b)$$

Since the time scale for  $\eta$  to approach its mean value is significantly shorter than the time scales for the changes in  $\lambda$  ( $\omega_{\lambda} / \omega_{\eta} \sim \lambda |k| \ll 1$ ) in the long-wave limit, we can set  $\eta \approx \eta_0$  in

Eq. (17). As a result we find from (17), using  $\langle \dot{\lambda} \rangle = 0$ , an equation for the rate of change of  $\lambda$ :

$$\frac{d\lambda}{dt} = \frac{V(C_{L\alpha} - C_{L\beta})}{\Gamma_{\alpha} + \Gamma_{\beta}} \left[ - \frac{(\Lambda_0 - 1)\Lambda^2}{\langle \Lambda^2 \rangle} + \Lambda - 1 \right] \quad (20a)$$

We also find an expression for the growth velocity:

$$V = V(\Lambda_0) \Lambda_0^2 / \langle \Lambda^2 \rangle, \quad (20b)$$

where  $\Lambda = \lambda / \lambda_c$ , and  $V(\Lambda_0)$  is given by (19a). When the variance of  $\Lambda$  is small, and the relation  $\langle \Lambda^2 \rangle \approx \Lambda_0^2$  holds, we find

$$\frac{d\Lambda}{dt} = \frac{V(C_{L\alpha} - C_{L\beta})}{(\Gamma_{\alpha} + \Gamma_{\beta})} \frac{(\Lambda_0 - 1)}{\Lambda_0^2} (\Lambda - \Lambda_0) \left( \frac{\Lambda_0}{\Lambda_0 - 1} - \Lambda \right) \quad (20c)$$

and  $V = V(\Lambda_0)$ , as for a regular eutectic. Equation (20c) has two stationary points: at  $\Lambda = \Lambda_0$  and at  $\Lambda = \Lambda_0 / (\Lambda_0 - 1)$ . At  $\Lambda_0 > 2$ , one stationary point is stable, while the other is unstable.

### SELECTION OF STRUCTURE

In the preceding section we derived Eq. (20) for the rate of change of the size of the lamella in the long-wave approximation. We will use that equation here to analyze the process by which a structure is selected. In addition to the governing equation of motion we will need to consider fluctuations in the system and the processes by which lamellae appear and disappear (Fig. 2b). To describe these processes we introduce the size distribution of the lamellae,  $f(\lambda, t)$ , which obeys a Fokker-Planck equation with a source:

$$\frac{\partial f}{\partial t} + \frac{\partial}{\partial \lambda} \left[ \dot{\lambda} f - B \frac{\partial f}{\partial \lambda} \right] = I(\lambda). \quad (21)$$

This distribution function is defined in such a way that  $f d\lambda$  is the number of lamellae in the interval from  $\lambda$  to  $\lambda + d\lambda$  per unit length of the front. It has been normalized by the natural condition

$$\int_0^{\infty} \lambda f d\lambda = 1. \quad (22)$$

In Eq. (21),  $\dot{\lambda}$  is determined by Eq. (20), and the diffusion coefficient  $B$  refers to the size diffusion of the lamella. It is proportional to the effective temperature and is assumed to be independent of  $\lambda$ . The source  $I(\lambda)$  arises from the splitting of lamellae. We denote by  $W(\lambda', \lambda'')$  the probability per unit time for a lamella of size  $\lambda'$  to split into two lamellae with sizes  $\lambda''$  and  $\lambda' - \lambda''$ . We can then write

$$I(\lambda) = \int_{\lambda}^{\infty} f(\lambda') W(\lambda', \lambda) d\lambda' - f(\lambda) \int_0^{\lambda/2} W(\lambda, \lambda'') d\lambda''. \quad (23)$$

Datye *et al.*<sup>9</sup> used a model in which a lamella splits in half when it reaches a certain critical size  $\lambda_d$ . In this case we would have

$$I(\lambda) = 2j_d \delta \left( \lambda - \frac{\lambda_d}{2} \right), \quad (24)$$

where  $j_d$  is the flux of lamella with  $\lambda = \lambda_d$ , and  $\delta$  is the Dirac  $\delta$ -function. This critical splitting can be linked with an instability of the crystallization front<sup>4</sup> when the lamellae are large. We will postpone for a moment an evaluation of  $\lambda_d$  for this splitting mechanism. At this point we wish to examine

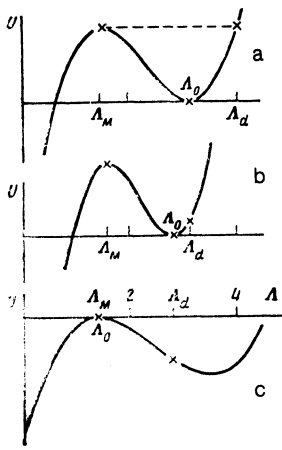


FIG. 3. The potential  $U(\lambda)$  in three possible cases. a— $\Lambda_d/2 > \Lambda_M$ ; b— $\Lambda_d/2 = \Lambda_M$ ; c— $\Lambda_d/2 = \Lambda_M = \Lambda_0$ . In cases a and b, the mean period of the structure,  $\Lambda_0$ , coincides with the point at which the potential reaches a minimum; in case c, it coincides with a maximum of the potential.

the steady-state solution of Eq. (21) with the source  $I(\lambda)$  from (24) and with the boundary conditions  $f(0) = f(\lambda_d) = 0$ :

$$f(\lambda) = \frac{j_d}{B} e^{-U(\lambda)/B} \int_0^\lambda e^{U(\lambda')/B} d\lambda' \quad \text{for } \lambda < \frac{\lambda_d}{2},$$

$$f(\lambda) = \frac{j_d}{B} e^{-U(\lambda)/B} \int_\lambda^{\lambda_d} e^{U(\lambda')/B} d\lambda' \quad \text{for } \lambda > \frac{\lambda_d}{2},$$
(25)

where  $U(\lambda) = -\int \lambda d\lambda$  is a potential which has extrema coinciding with the stationary points of Eq. (20) (Fig. 3). The constant  $j_d$  is found from normalization condition (22). The condition that  $f(\lambda)$  is continuous at  $\lambda = \lambda_d/2$  can be used to determine the value of  $\lambda_0$ , on which the potential  $U(\lambda)$  depends parametrically.

A. Low noise level. In the limit  $B \rightarrow 0$  the condition that  $f(\lambda)$  is continuous can be written as follows for  $\lambda = \lambda_d/2$ :

$$U(\lambda_-) = U(\lambda_+),$$
(26)

where  $\lambda_-$  and  $\lambda_+$  correspond to the highest values of the potential in the regions  $\lambda < \lambda_d/2$  and  $\lambda > \lambda_d/2$ . There are two possibilities here.

1)  $\lambda_d/2 > \lambda_M$ , where  $\lambda_M$  is the coordinate of the potential maximum (Fig. 3a). In this case we have  $\lambda_+ = \lambda_d$  and  $\lambda_- = \lambda_M$ , and Eq. (26) leads to the solution

$$\Lambda_0 = \frac{1}{5} [\Lambda_d + 2 + (\Lambda_d^2 - 2\Lambda_d + 4)^{1/2}],$$
(27)

which exists if  $\Lambda_d \geq 16/5$ .

2)  $\lambda_d/2 = \lambda_M$ . In this case we have  $\lambda_- = \lambda_d/2$ ,  $U(\lambda_d) < U(\lambda_d/2)$ , and thus  $\lambda_+ = \lambda_d/2$ . This situation holds if  $\Lambda_d \leq 16/5$ , and if  $\Lambda_0$  is found from the equation  $\Lambda_M = \Lambda_d/2$ . In the solution of this equation there are two possible cases:

$$\Lambda_0 = \Lambda_d / (\Lambda_d - 2) \quad \text{for } 3 \leq \Lambda_d \leq 16/5,$$
(28)

$$\Lambda_0 = \Lambda_d / 2 \quad \text{for } 2 \leq \Lambda_d < 3.$$
(29)

Solution (28) corresponds to the case in which  $\Lambda_0$  coincides

with a minimum of the potential  $U$  (Fig. 3b), while for solution (29)  $\Lambda_0$  coincides with a maximum of  $U$  (Fig. 3c).

At  $\Lambda_d \geq 3$  the value found for  $\Lambda_0$  thus corresponds to a minimum of  $U$  (Fig. 3, a and b). This result means that at a low noise level there is actually a regular stable structure with a period  $\Lambda_0$  (with a sharp Gaussian distribution function near  $\Lambda_0$ ). Events in which lamellae split and collapse occur exponentially rarely in such a structure and maintain the given steady state.

For  $2 < \Lambda_d < 3$ , solution (29) holds, for which  $\Lambda_0$  corresponds to a maximum of the potential  $U$ . Lamellae smaller than the mean size decrease and ultimately collapse, while lamellae of size greater than the mean increase; when they reach a size  $\Lambda_d$ , they split. In contrast with the preceding case, the splitting and collapse processes do not require the attainment of certain dimensions by means of fluctuations. The rates of these processes do not contain an exponentially small factor, and the distribution function is a power law.

In the limit  $B \rightarrow 0$ , distribution function  $f(\lambda)$  for solutions (27) and (28) is concentrated near  $\Lambda_0$ . If there is even a small probability for the splitting of such lamellae, then it will be primarily the lamellae with a size close to  $\Lambda_0$  which split. This statement means that we should set  $\Lambda_d = \Lambda_0$ . We then find from (28)

$$\Lambda_0 = 3.$$
(30)

This universal result does not depend on the parameters characteristic of the fluctuations and of the splitting of lamellae. The same result could be obtained by solving Eq. (21) with a source of a general type as in (23); i.e., we could discard our model assumption of a splitting precisely in half at the size  $\Lambda_d$ .

For simplicity we assume that the splitting of the lamellae occurs in arbitrary proportions with equal probability, i.e., that the function  $W(\lambda', \lambda'')$  does not depend on its second argument. Under the assumption that in the limit  $B \rightarrow 0$  the distribution function is localized near  $\lambda_0$  and that the function  $W$  is smoother, we find the following expression for the source  $I(\lambda)$  from (23):

$$I(\lambda) = -f(\lambda) W(\lambda) \frac{\lambda}{2} + \begin{cases} W(\lambda_0)/\lambda_0 & \text{for } \lambda \leq \lambda_0, \\ 0 & \text{for } \lambda > \lambda_0. \end{cases}$$

Solving the steady-state Equation (21) with this expression for the source, and without a flux at large values of  $\lambda$ , we find the following expression for the function  $f(\lambda)$ :

$$f(\lambda) = \frac{W(\lambda_0)}{2B\lambda_0} e^{-U(\lambda)/B} \int_0^\lambda (\lambda_0 - 2\lambda') e^{U(\lambda')/B} d\lambda' \quad \text{for } \lambda \leq \lambda_0.$$
(31)

For  $\lambda > \lambda_0$  the distribution function is described by the same expression, except that the upper limit of  $\lambda$  on the integral is replaced by  $\lambda_0$ . The value  $\lambda_0$  in which we are interested is found from normalization condition (22). Near  $\lambda_0$ , the distribution function is

$$f(\lambda) \sim \exp \left[ \frac{U(\lambda_M) - U(\lambda)}{B} \right] (\lambda_0 - 2\lambda_M).$$

In the limit  $B \rightarrow 0$  the first factor increases rapidly, so that the normalization condition can be satisfied only if the expression in parentheses vanishes. We thus find

$$\lambda_0 = 2\lambda_M = 2\lambda_0 / [\lambda_0 / \lambda_c - 1] \quad \text{or} \quad \lambda_0 = 3\lambda_c,$$

in agreement with (30).

**B. Evaluation of  $\lambda_d$ .** The splitting of the lamellae occurs through the formation, ahead of a lamella of one of the phases (say  $\beta$ ), of a lamella of the other phase ( $\alpha$ ). This process is facilitated when a splitting lamella reaches a certain critical size<sup>4</sup>  $\lambda_{\beta d}$ , at which a deep concave section forms at the front, highly supersaturated with respect to the  $\alpha$  phase. As in Ref. 4, we define  $\lambda_{\beta d}$  as the size at which a point with a vertical slope,  $d\xi/dx = \infty$ , first appears at the  $\beta$  front. The front of a  $\beta$  lamella in this case clearly consists of three approximately identical regions, and the central concave region has a curvature on the order of  $6/\lambda_{\beta d}$ . Consequently, the curvature in the middle of the  $\beta$  lamella can be written as  $K = 6a_\beta/\lambda_{\beta d}$ , with a coefficient  $a_\beta$  on the order of 1; this coefficient may depend on the parameters  $\eta$  and  $\theta_S$ . In our long-wave approximation, the composition of the melt above the middle of the critical  $\beta$  lamella is  $C_L^\beta = \bar{C}_L = \bar{C}_L^\beta$ , where  $\bar{C}_L$  is the mean composition, given by (12b), and  $\bar{C}_L^\beta$  is calculated from the expressions for a regular eutectic with the parameters  $\eta_0$ ,  $\lambda = \lambda_d \equiv \lambda_{\beta d} / (1 - \eta_0)$ ,  $V$ :

$$\bar{C}_L^\beta = -(C_\beta^E - C_\alpha^E) Q(1 - \eta_0) V \lambda_d / D, \quad (32a)$$

$$Q(1 - \eta_0) = \sum_{n=1}^{\infty} \frac{\sin \pi n (1 - \eta_0)}{(\pi n)^2}. \quad (32b)$$

Substituting this composition and the curvature into the equilibrium equation (3b), we find

$$\begin{aligned} & \eta_0 (C_{L\alpha} - C_{L\beta}) (1 - \lambda_c / \lambda_0) - (C_\beta^E - C_\alpha^E) Q(1 - \eta_0) V \lambda_d / D \\ &= - \frac{2\Gamma_\beta}{(1 - \eta_0)} \left( \frac{3a_\beta}{\lambda_d} + \frac{\theta_\beta}{\lambda_0} \right). \end{aligned} \quad (33)$$

Here we have used expressions (12b) and (19b) for  $\bar{C}_L$  and  $\lambda_c$ . Comparing (33) with the results of the numerical calculation of  $\lambda_d$  which was carried out in Ref. 4 for a regular eutectic with  $\lambda_0 = \lambda_d$  and with  $\eta_0 = 0.1$  and  $0.5$ , and using a very simple interpolation formula for the function  $a_\beta$  ( $\eta_0$ ,  $\theta_\beta$ ), we find

$$a_\beta = 0.72 + 0.11\eta_0 + (0.33 - 0.42\eta_0) \sin \theta_\beta. \quad (34)$$

As expected, the coefficient  $a_\beta$  is close to 1 in order of magnitude. Jackson and Hunt<sup>4</sup> considered the case of finite—not small—values of  $\theta_\beta$ . In the case at hand, we should replace  $\sin \theta_\beta$  simply by  $\theta_\beta$ . In (33) we replace  $V$  by its expression in terms of  $\lambda_0$ , (20b). We also consider systems with identical surface energies  $\sigma_{L\alpha} = \sigma_{L\beta}$  for which we have  $\theta_\alpha = \theta_\beta = \theta$  and, according to (3c),

$$\Gamma_\alpha = \gamma / (1 - \eta_E), \quad \Gamma_\beta = \gamma / \eta_E.$$

Here  $\gamma$  can be expressed in terms of  $\lambda_c$  [see (19b)]. Here

$$\eta_E = (C_\beta^E - C_L^E) / (C_\beta^E - C_\alpha^E)$$

is the fraction of the  $\alpha$  phase in the eutectic composition. In this case we find from (33) and (20b)

$$\begin{aligned} & M(1 - \eta_0) \frac{\Lambda_d^2}{\langle \Lambda^2 \rangle} (\Lambda_0 - 1) - \eta_0 \frac{\Lambda_d}{\Lambda_0} (\Lambda_0 - 1) \\ & - \frac{\eta_0 (1 - \eta_E)}{(\eta_0 + \eta_E - 2\eta_0 \eta_E)} \left( \frac{\Lambda_d}{\Lambda_0} + \frac{3a_\beta}{\sin \theta} \right) = 0. \end{aligned} \quad (35)$$

$M(1 - \eta) = \eta(1 - \eta)Q(1 - \eta)/P(\eta)$ . Expressions (34) and (35) were derived for the splitting of a  $\beta$  lamella. If  $\alpha$  lamellae are splitting, then we can find the corresponding expression for  $a_\alpha$  from (34) by replacing  $\theta_\beta$  by  $\theta_\alpha$  and replacing  $\eta_0$  by  $1 - \eta_0$ ; we find an equation for  $\Lambda_d$  from (35) by replacing  $\lambda_0$  by  $1 - \eta_0$  and by replacing  $\eta_E$  by  $1 - \eta_E$ .

Solving Eq. (35) and Eqs. (27)–(29) simultaneously in the low-noise-level limit determines the mean period of the structure,  $\Lambda_0$ , and that value of this period ( $\Lambda_d$ ) at which the lamellae split in this structure.

a. For a solution of type (27),  $\Lambda_0$  is the larger of the roots of the quadratic equation

$$\begin{aligned} & \Lambda_0^2 (9M - 6\eta_0) - \Lambda_0 \left( 24M + 6H + \frac{12Ha_\beta}{\sin \theta} - 14\eta_0 \right) \\ & + 16M + 8H + \frac{12Ha_\beta}{\sin \theta} - 8\eta_0 = 0, \end{aligned}$$

$$\Lambda_d = \frac{\Lambda_0 (3\Lambda_0 - 4)}{2(\Lambda_0 - 1)} \quad \text{and} \quad \Lambda_d > \frac{16}{5}.$$

b. For a solution of type (28), we have

$$\Lambda_0 = 1 + \frac{2M - H}{\eta_0 + 3Ha_\beta / 2 \sin \theta},$$

$$\Lambda_d = \frac{2\Lambda_0}{\Lambda_0 - 1} \quad \text{and} \quad 3 \leq \Lambda_d \leq \frac{16}{5}.$$

c. For a solution of type (29) we have

$$\Lambda_0 = 1 + \frac{H + 3Ha_\beta / 2 \sin \theta}{2M - \eta_0}, \quad \Lambda_d = 2\Lambda_0 \quad \text{and} \quad 2 \leq \Lambda_d < 3.$$

Here

$$H = \eta_0 (1 - \eta_E) / (\eta_0 + \eta_E - 2\eta_0 \eta_E)$$

and  $M \equiv M(1 - \eta_0)$ . Figure 4 shows some results calculated from these expressions. The curves of  $\Lambda_0$  and  $\Lambda_d$  versus  $\eta$  in Fig. 4, a and b, are symmetric with respect to the composition  $\eta = 0.5$ . In the case of the alloys of the eutectic composition  $\eta_0 = \eta_E$  (Fig. 4a),  $\alpha$  lamellae split at  $0 < \eta_E < 0.5$ , while  $\beta$  lamellae split at  $0.5 < \eta_E < 1$ . In the case of the symmetric eutectic,  $\eta_E = 0.5$  (Fig. 4b),  $\beta$  lamella split at  $0 < \eta_0 < 0.5$ , and  $\alpha$  lamellae at  $0.5 < \eta_0 < 1$ .

For the eutectic with  $\eta_E = 0.2$  (Fig. 4c),  $\beta$  lamellae split at  $0 < \eta_0 < 0.15$ , and  $\alpha$  lamella at  $0.15 < \eta_0 < 1$ .

**C. Effect of the noise level.** At a nonzero noise level, two important effects arise. First, all of the sharp transitions (the changes in slope and jumps in Fig. 4) from one growth regime to another become smeared out. Second, as the noise increases or (equivalently) as the variance in the thicknesses of the lamellae increases, the mean structural period  $\Lambda_0$  decreases. Figure 5 shows the results of a numerical calculation of  $\Lambda_0$  and  $\Lambda_d$  as functions of the variance of the structure for the eutectic composition  $\eta_0 = \eta_E = 0.38$ , which corresponds to the Pb-Sn system.

To find the three quantities  $\Lambda_0$ ,  $\Lambda_d$ , and the variance for a given  $B$ , we make use of the following:

- 1) The continuity condition for the distribution function (25) with  $\Lambda = \Lambda_d / 2$ .
- 2) The definition of  $\Lambda_0$ ,

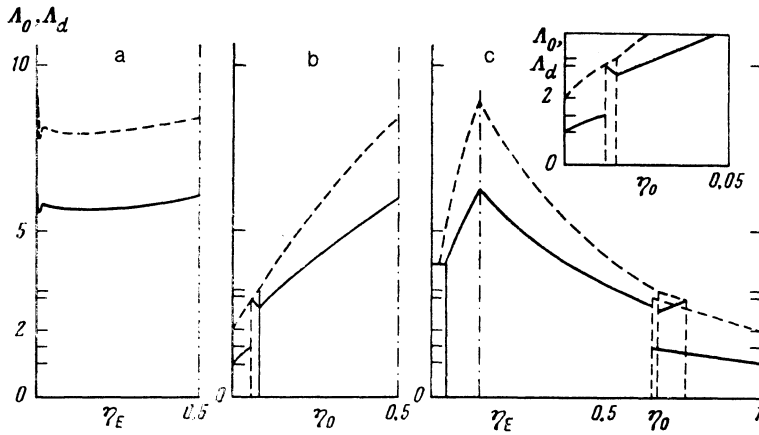


FIG. 4. The mean lamellar spacing  $\Lambda_0$  and the distance at which a lamella splits,  $\Lambda_d$ , versus  $\eta_0$ , which is the fraction of the  $\alpha$  phase in the crystallizing structure. These results were found for equal surface energies,  $\sigma_{L\alpha} = \sigma_{L\beta}$ , with  $\theta_\alpha = \theta_\beta = \pi/6$ . Solid curves— $\Lambda_0$ ; dashed curves— $\Lambda_d$ . a:  $\eta_0 = \eta_E$ . Throughout the region  $0 < \eta_E < 0.5$ ,  $\alpha$  lamellae split, and the case shown in Fig. 3a prevails. b:  $\eta_E = 0.5$ . Throughout the region  $0 < \eta_0 < 0.5$ ,  $\beta$  lamellae split. As  $\eta_0$  increases, the cases shown in Fig. 3 occur in the order c, b, a. c:  $\eta_E = 0.2$ . In the region  $0 < \eta_0 < 0.15$ ,  $\beta$  lamellae split, while at  $0.15 < \eta_0 < 1$  the  $\alpha$  lamellae split. On the right side of the figure there are two regions of  $\eta_0$  with two solutions.

$$\Lambda_0 = \int_0^\infty \Lambda f d\Lambda / \int_0^\infty f d\Lambda$$

(under these two conditions, the relation

$$\langle \Lambda^2 \rangle = \int_0^\infty \Lambda^2 f d\Lambda / \int_0^\infty f d\Lambda$$

in fact becomes a consequence of the Fokker-Planck equation).

3) Equation (35), which determines the stability boundary  $\Lambda_d$ .

In calculating the potential  $U(\Lambda)$  and the growth rate  $V(\Lambda)$ , we use the general relations (20a) and (20b). At high temperatures ( $B \rightarrow \infty$ ), we can ignore in Eq. (21) the term containing  $\lambda$ . It then becomes a simple matter to find analytically that the variance tends toward a finite limit  $\langle (\Lambda - \Lambda_0)^2 \rangle / \Lambda_0^2 = 1/6$ , and we have  $\Lambda_0 = \Lambda_d/2$ . For the system under consideration here (Fig. 5), this limiting value is  $\Lambda_0 = 3.4$ .

## DISCUSSION

We have used the long-wave approximation to describe the dynamic evolution of the structure. This approximation is clearly an imperfect representation of the actual situation since, at least immediately after the splitting or collapse of a lamella, the distortions of the structure are not long-wave

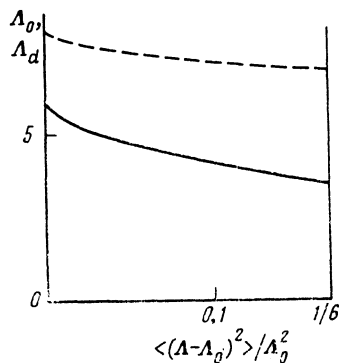


FIG. 5.  $\Lambda_0$  (solid line) and  $\Lambda_d$  (dashed line) versus the variance in the periods of the structure for  $\eta_0 = \eta_E = 0.38$  ( $\sigma_{L\alpha} = \sigma_{L\beta}$  and  $\theta_\alpha = \theta_\beta = \pi/6$ ).

distortions. On the other hand, the net role of the appearance and disappearance processes reduces to one of decreasing or increasing the period of the eutectic structure. In other words, the net role is ultimately one of causing long-wave changes in the structure. The “short-wave” splitting events, on the other hand, are dealt with by introducing a source in the Fokker-Planck equation.

In contrast with Ref. 9, we have not considered any curvature of the macroscopic front. It follows from the linear stability analysis in Ref. 11 that the curvature of the macroscopic front can be ignored if  $k\lambda \gg \theta_S$ . Since we have  $\theta_S \sim \sigma_{\alpha\beta} / \sigma_{LS}$ , in systems with  $\sigma_{LS} \gg \sigma_{\alpha\beta}$  the long-wave approximation has a wide range of applicability,  $1 \gg k\lambda \gg \theta_S$ , at a plane macroscopic front. Since the macroscopic front remains planar in our approximation, we have used no additional assumptions of any sort regarding the perpendicular orientation of the lamellae with respect to the line of the macroscopic front. In this regard our study stands in contrast with Ref. 9. There are experimental indications, shown in Fig. 5 of Ref. 8, that the macroscopic front does remain planar, despite the large scatter in the sizes of the lamellae.

Kirkaldy<sup>8</sup> concluded from considerations of the stability of a structure with regard to perturbations of a certain type that the structure which is selected is that which corresponds to the inflection point on the  $V(\Lambda)$  curve. For the function  $V(\Lambda)$  in (19a), that result agrees with our universal result (30):  $\Lambda_0 = 3$ . This agreement, however, should be judged fortuitous, since the physical reasoning is different. According to our reasoning, this result corresponds to the condition  $V(\Lambda) = V(\Lambda_0/2)$ , and it does not coincide with the inflection point for a more general function  $V(\Lambda)$ .

We have been studying the growth of a eutectic structure under isothermal conditions here. Essentially all of the results, however, can be extended to the case of growth in a temperature gradient, provided that the temperature drop over a length scale  $\lambda_0$  is much smaller than the supercooling required for the growth at the given velocity  $V$  and at the given lamella size  $\lambda_0$ . This condition usually holds quite well. In this case Eq. (19a) determines the supersaturation  $\Delta C \equiv C_{L\alpha} - C_{L\beta}$  (and thus the supercooling). During growth in a temperature gradient, the mean size of the lamellae which emerges as a result of the selection processes can be expressed more conveniently in terms of the characteristic dimension corresponding to the minimum of the supersaturation  $\Delta C(\lambda)$  from (19a) at a given growth velocity  $V$ , rather

than in terms of the size  $\lambda_c$ . This switch is made with the formula

$$\lambda_0/\lambda_m = (\lambda_0/\lambda_c - 1)^{1/2}. \quad (36)$$

The universal low-temperature result  $\lambda_0 = 3\lambda_c$  from the isothermal case thus takes the following form in the case of a temperature gradient:

$$\lambda_0 = 2^{1/2}\lambda_m.$$

This analysis shows that the mean value  $\Lambda_0$  which emerges as a result of the selection can lie anywhere in a certain interval of values, depending on the particular model used for the splitting of the lamellae. The upper boundary of this interval corresponds to the splitting of lamellae at  $\Lambda = \Lambda_d$ , i.e., at the point at which the front of the lamellae becomes unstable. In this case there is a very large increase in the supersaturation at a concave section of the front, and the barrier for the thermal-fluctuation nucleation of lamellae essentially disappears. Values of  $\Lambda_0$  corresponding to this upper boundary are shown in Fig. 4. In principle, splitting can also occur at smaller values of  $\Lambda$ , as a result of thermal-fluctuation nucleation; the result would be to reduce  $\Lambda_0$ . The minimum value of  $\Lambda_0$  is reached when the splitting of the lamellae occurs not near the point of instability but near the mean value  $\Lambda_0$ . This case corresponds to result (30):  $\Lambda_0 = 3$ . For the Pb-Sn eutectic with  $\eta_0 = \eta_E = 0.38$ , for example, we find  $3 \leq \lambda_0/\lambda_c \leq 5.84$ ; according to (36), this interval leads to  $2^{1/2} \leq \lambda_0/\lambda_m \leq 2.20$ . To compare this theoretical result with experimental data, we used data on the crystallization of a eutectic in thin films from Ref. 12. From Fig. 10 of that paper we found values of  $\lambda_0$  and  $V$ . The values of  $\lambda_m$  for

various values of  $V$  can be found from the formula  $\lambda_m = 4.82 \cdot 10^{-6} V^{-1/2}$  ( $\lambda$  is in centimeters and  $V$  in centimeters per second), which follows from experimental results.<sup>13</sup> The values found for  $\lambda_0/\lambda_m$  in different experiments differ widely; they fall in the interval 1.2–2.0. Significantly, the structures studied in those experiments were essentially defect-free; i.e., the fluctuation level was low. In such a situation the selection process may take a rather long time, and the observed structures may not correspond to the final steady state. If a selection process does not have time to occur, the structures which result may have periods which lie between two stability limits,<sup>4,12</sup>  $1 < \lambda_0/\lambda_m \leq 4$ .

We wish to thank S. V. Meshkov for useful discussions.

<sup>1</sup>J. S. Langer, *Rev. Mod. Phys.* **52**, 1 (1980).

<sup>2</sup>M. Kerszberg, *Phys. Rev.* **B28**, 247 (1983).

<sup>3</sup>J. W. Christian, *Theory of Transformations in Metals and Alloys*, Pergamon, New York, 1975 [Russ. transl., Mir, Moscow, 1978].

<sup>4</sup>K. A. Jackson and J. D. Hunt, *Trans. AIME* **236**, 1129 (1966).

<sup>5</sup>J. S. Langer, *Phys. Rev. Lett.* **44**, 1023 (1980).

<sup>6</sup>C. Zener, *Trans. AIME* **167**, 550 (1946).

<sup>7</sup>B. E. Sundquist, *Acta Met.* **16**, 1413 (1968).

<sup>8</sup>J. S. Kirkaldy, *Phys. Rev.* **B30**, 6889 (1984).

<sup>9</sup>V. Datye, R. Mathur, and S. J. Langer, *J. Stat. Phys.* **29**, 1 (1982).

<sup>10</sup>D. E. Temkin, *Kristallografiya* **30**, 1055 (1985) [*Sov. Phys. Crystallogr.* **30**, 671 (1985)].

<sup>11</sup>V. Datye and J. S. Langer, *Phys. Rev.* **B24**, 4155 (1981).

<sup>12</sup>H. E. Cline, *Met. Trans.* **15A**, 1013 (1984).

<sup>13</sup>R. M. Jordan and J. D. Hunt, *Met. Trans.* **3**, 1385 (1972).

Translated by Dave Parsons